



Article

Beamforming Optimization for Intelligent Reflecting Surface-Assisted MIMO Systems

Wenjuan Zhang ¹, Honggui Deng ^{1,*}, Youzhen Li ¹, Zaoxing Zhu ¹, Chengzuo Peng ¹ and Gang Liu ^{1,2}

¹ School of Physics and Electronics, Central South University, Changsha 410083, China; 202212099@csu.edu.cn (W.Z.); liyouzhen@csu.edu.cn (Y.L.); csuzzx970112@csu.edu.cn (Z.Z.); 202212087@csu.edu.cn (C.P.); 162201003@csu.edu.cn (G.L.)

² College of Information Science and Engineering, Changsha Normal University, Changsha 410100, China

* Correspondence: denghonggui@csu.edu.cn

Abstract: To improve the spectral efficiency of symmetry-based intelligent reconfigurable surface (IRS)-assisted MIMO communication systems, this paper investigates the joint precoding and passive beamforming optimization problem for millimeter-wave point-to-point MIMO systems under both ideal and practical IRS phase shifts. For the ideal IRS phase shifts setup, we derive a simplified approximate spectral efficiency expression based on Jensen's inequality and propose a minimum mean square error (MMSE)-based algorithm to transform the simplified non-convex problem into a solvable convex function. For the practical IRS phase shifts setup, we propose a multi-start stepwise optimization algorithm to obtain the passive beamforming by stepwise iterative search. Finally, with the above-obtained passive beamforming, the optimal precoding is derived by performing the singular value decomposition (SVD) on the effective channel and water-filling power allocation. The simulation results verify our performance analysis and demonstrate that spectral efficiency can be effectively improved compared to various benchmark schemes.

Keywords: intelligent reflecting surface; MIMO; beamforming optimization; discrete phase shifts; spectral efficiency



Citation: Zhang, W.; Deng, H.; Li, Y.; Zhu, Z.; Peng, C.; Liu, G. Beamforming Optimization for Intelligent Reflecting Surface-Assisted MIMO Systems. *Symmetry* **2022**, *14*, 1510. <https://doi.org/10.3390/sym14081510>

Academic Editors: Haitao Xu, Chin-Ling Chen and José Carlos R. Alcántud

Received: 21 June 2022

Accepted: 20 July 2022

Published: 23 July 2022

Publisher's Note: MDPI stays neutral with regard to jurisdictional claims in published maps and institutional affiliations.



Copyright: © 2022 by the authors. Licensee MDPI, Basel, Switzerland. This article is an open access article distributed under the terms and conditions of the Creative Commons Attribution (CC BY) license (<https://creativecommons.org/licenses/by/4.0/>).

1. Introduction

Millimeter-wave MIMO systems can effectively overcome the free-space path loss problem by employing beamforming techniques to achieve higher spectral efficiency; however, a large number of antenna elements and radio frequency (RF) chains will inevitably generate significant overhead and power consumption [1,2]. The intelligent reflecting surface (IRS), with its increased potential for significant energy consumption reductions, has become a green and cost-effective solution [3,4]. Specifically, an IRS is a large electromagnetic metasurface consisting of metals, dielectrics, and tunable elements that can realize the real-time amplitude/phase adjustment of the incident electromagnetic wave signal through adjusting the physical properties of electromagnetic elements, such as capacitive, impedance, or inductive resistance, to achieve three-dimensional spatial beamforming and improve the performance of the communication system [5,6]. When the direct communication link between the base station (BS) and the user is blocked by an obstacle, the BS can align the transmitting beam to the IRS, and then the IRS can align the reflected beam to the user by adjusting the phase of the array elements so that a good communication performance can still be maintained between the BS and the user. In addition, the IRS can be deployed on indoor ceilings, walls, or building facades, bringing great flexibility to wireless systems [7].

There are two technical difficulties in the beamforming optimization of an IRS-assisted millimeter wave MIMO system. One is the deep coupling between the precoding and the passive beamforming of the IRS in the spectral efficiency maximization objective problem, which makes it extremely difficult to solve the joint optimization problem. The other is that

the reflection element of an IRS is subject to strict instantaneous power limitations, that is, non-convex unit modulus constraints, which makes the spectral efficiency optimization problem non-convex and difficult to solve.

Based on the above issues, several previous works have focused on beamforming optimization for IRS-assisted communication systems. The researchers in [8] investigated the problem of maximizing the spectral efficiency of IRS-assisted MIMO communication systems but did not consider joint optimization with active beamforming. The researchers in [9] jointly optimized the precoding at the BS and the passive beamforming at the IRS, and transformed it into convex semidefinite planning (SDP) problem, which is solved by the semi-definite relaxation technique (SDR), but the computational complexity is high. In view of the high computational complexity of the SDR algorithm, the researchers in [10] first simplified the objective problem using fractional programming techniques and then obtained an approximate optimal solution based on the block coordinate descent (BCD) method. The researchers in [11] focused on the maximization of channel capacity in point-to-point MIMO systems, which is approximately transformed into the maximization of total channel gain. An effective alternating iterative method is developed to obtain the local optimal solution of passive beamforming, but the spectral efficiency is not ideal. In addition, the above literature is based on the ideal IRS with a continuous phase shifts setup, and due to the manufacturing process and hardware limitations, the reflection phase of the practical IRS can only obtain a certain number of specific discrete values. Although the researchers in [12] considered the practical IRS with finite resolution phase shifters, it directly quantifies the optimal continuous phase shift to the discrete phase shift domain, which is bound to bring non-negligible errors when the resolution accuracy is low. In [13], the non-convex spectral efficiency optimization problem of the MIMO system assisted by an IRS with discrete phase shifts was transformed into a discrete phase search problem, but the optimal phase shifts of all reflection elements are obtained by an exhaustive search, and this algorithm is highly unsuitable when the reflection elements are large. In particular, considering the propagation characteristics of millimeter-waves, the simulation based on the Rayleigh fading channel or Rician fading channel in the above literature is not realistic.

Based on the above analysis, most of the existing IRS-assisted beamforming optimization work for MIMO systems cannot obtain the desired spectral efficiency, and some have the problem of high computational complexity and limitations of application scenarios. How to effectively solve the non-convex spectral efficiency problem caused by the non-convex, single-mode constraint and how to jointly optimize the precoding and passive beamforming are the keys to improving the spectral efficiency. In order to maximize the spectral efficiency of the IRS-assisted millimeter-wave MIMO system when the BS–user direct path is blocked, this paper proposes beamforming schemes for the ideal IRS with a continuous phase shifts setup and for the practical IRS with a discrete phase shifts setup, respectively. The contributions of this paper can be summarized as follows:

- For the complex spectral efficiency optimization problem in an ideal IRS, the original spectral efficiency optimization problem is transformed into an effective channel gain maximization problem based on Jensen's inequality, which is easier to solve.
- For the effective channel gain maximization problem with non-convex single-mode constraints, a passive beamforming scheme based on an MMSE is proposed in this paper, and it transforms the non-convex optimization problem into a minimum mean square error problem of the optimal solution and the actual matrix, and, further, the closed solution is obtained.
- For the non-convex spectral efficiency optimization problem in a practical IRS, this paper proposes a multi-start, stepwise optimization scheme, which transforms the beamforming at the IRS into a phase search problem. Multiple starting points are generated through chaotic mapping, and the optimal discrete phase shift of the IRS is obtained by iterative steps, which greatly reduces the complexity.

The remainder of this paper is organized as follows: Section 2 presents the system model and the problem formulation. Then, Section 3 proposes two beamforming optimiza-

tion schemes for solving the formulated problem under different IRS setups. Section 4 provides the numerical results and their pertinent discussions. Finally, we summarize the full paper in Section 5.

2. System Model and Problem Formulation

In this section, the IRS-assisted point-to-point MIMO communication system model, channel model, and optimization problem are established.

2.1. System Model

The architecture of an IRS-assisted point-to-point MIMO communication system is shown in Figure 1, where the BS is equipped with N_t antennas and the number of data streams is N_s , with $N_s \leq N_t$. The data streams are first modulated by the precoder F and then reflected by the IRS attached to the wall, where the IRS is equipped with M reflection elements to serve the user equipped with N_r antennas. The IRS equipped with a controller can dynamically adjust the reflection coefficient based on the propagation environment learned through periodic sensing via the same passive array (when not reflecting). Due to significant path loss, we assume that each element at the IRS can re-scatter the signal independently, and the signals which are reflected twice or more are ignored. Furthermore, the direct BS–user path is blocked due to obstacles and severe path loss, the BS–IRS and IRS–user paths have already known the perfect channel state information (CSI) through channel estimation and effective feedback techniques, and the IRS controller communicates with the BS through a separate radio link for the CSI exchange. The specific channel estimation techniques have been studied in various works [14–16]. Thus, the received signal of the BS–IRS–user path is expressed as:

$$y = \sqrt{\frac{P}{N_s}} (H_r \Phi G F s) + z \quad (1)$$

where P is the total transmit power and $z \in \mathbb{C}^{N_r \times 1}$ is the noise vector, which obeys complex Gaussian distribution with a 0 mean and $\sigma^2 I_{N_r}$ covariance, where σ^2 denotes the average noise power and I_{N_r} denotes the N_r -dimensional unit matrix. The input signal $s \in \mathbb{C}^{N_s \times 1}$ satisfies $\mathbb{E}[ss^H] = \frac{P}{N_s} * I_{N_s}$, where the $\mathbb{E}[\cdot]$ unit is a statistical expectation and $*$ denotes a multiplication. $F \in \mathbb{C}^{N_t \times N_s}$ is the precoding matrix satisfying $\|F\|_F^2 = N_s$, and, due to the symmetric structure of the precoding system, the combiner at the receiver side can be designed similarly to the precoder at the transmitter side, and so we omit it and focus on the design of the precoding. The IRS combines all the received multi-path signals at the BS, and re-scatters the combined signal. $\Phi = \text{diag}(\beta e^{j\theta_1}, \beta e^{j\theta_2}, \dots, \beta e^{j\theta_M}) \in \mathbb{C}^{M \times M}$ is the diagonal passive beamforming matrix at the IRS, where $\theta_i \in [0, 2\pi]$, $i = 1, 2, \dots, M$ is the phase of passive beamforming matrix and $\beta \in [0, 1]$ is the amplitude, and, generally, we set to $\beta = 1$. However, in practical process manufacturing, the phase of the IRS can only take a certain number of specific discrete values, and we set θ to belong to $\Gamma = \{0, \Delta\theta, \dots, \Delta\theta(2^b - 1)\}$, where $\Delta\theta = 2\pi/2^b$, b is the number of bits quantized. $H_r \in \mathbb{C}^{N_r \times M}$ and $G \in \mathbb{C}^{M \times N_t}$ denote the BS–IRS and IRS–user channels, respectively.

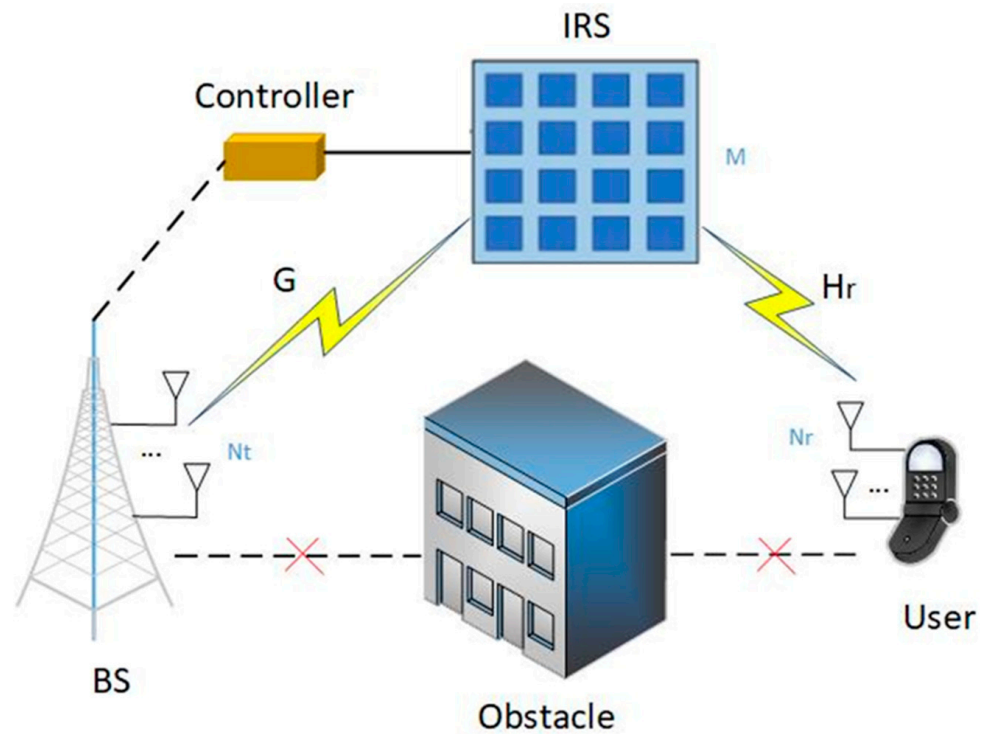


Figure 1. IRS-assisted point-to-point MIMO communication system with N_t BS antennas, N_r user antennas, and M IRS elements.

Since the high free-space path loss of the millimeter-wave channel leads to finite spatial selectivity or scattering, the channel model used in a conventional MIMO is no longer applicable for millimeter-wave MIMO systems, and we adopt the geometric Saleh–Valenzuela channel model [17,18]. We set the antennas at the BS to employ a uniform linear array (ULA) and the antennas at the IRS to employ a uniform planar array (UPA), and then the BS–IRS channel can be expressed as:

$$G = \sqrt{\frac{N_t N_r}{N_{cl} N_{ray}}} \sum_{i=1}^{N_{cl}} \sum_{l=1}^{N_{ray}} \alpha_{il} a_r(\phi_{r,l}, \psi_{r,l}) a_t(\theta_{t,l})^H \quad (2)$$

where N_{cl} is the number of scattering clusters, N_{ray} is the number of paths in each cluster, and α_{il} is the complex gain of the l -th path in the i -th scattering cluster and follows the complex Gaussian distribution, which is usually assumed to be 1. $a_r(\phi_{r,l}, \psi_{r,l})$ and $a_t(\theta_{t,l})$ denote the antenna array response vectors at the receiver and transmitter, respectively, where $\phi_{r,l}$, $\psi_{r,l}$, and $\theta_{t,l}$ are the azimuth angles of departure (AoD), the zenith angles of departure (ZoD), and the azimuth angles of arrival (AoA), respectively, and the array response vectors are expressed as follows:

$$a_t(\theta) = \frac{1}{\sqrt{N_t}} \left[1, e^{j\frac{2\pi}{\lambda} d \sin(\theta)}, \dots, e^{j\frac{2\pi}{\lambda} (N_t-1) d \sin(\theta)} \right]^T \quad (3)$$

$$a_r(\phi, \psi) = \frac{1}{\sqrt{N_r}} \left[1, \dots, e^{j\frac{2\pi}{\lambda} d (\alpha \sin(\phi) \sin(\psi) + \beta \cos(\psi))}, \dots, e^{j\frac{2\pi}{\lambda} d ((\sqrt{N_r-1}) \sin(\phi) \sin(\psi) + (\sqrt{N_r-1}) \cos(\psi))} \right]^T \quad (4)$$

where λ is the wavelength and d indicates the antenna spacing. In addition, the central angle of the cluster is uniformly distributed in the angular domain and the angular expansion of the multipath components in the cluster follows the Laplace distribution. Further, the IRS–user channel is modeled similarly to the BS–IRS channel.

Based on Shannon's theorem, the spectral efficiency (SE) can be presented as:

$$SE = \log_2 \det \left(I_{N_r} + \frac{P}{\sigma^2 N_s} H_{eff}^H F F^H H_{eff} \right) \quad (5)$$

where the effective channel $H_{eff} = H_r \Phi G$ is the BS-IRS-user channel. $\det(\cdot)$ and $(\cdot)^H$ are the conjugate transpose of the matrix and operation of the determinant of a matrix, respectively. In order to maximize the spatial multiplexing gain of the MIMO, we set $N_s = \text{rank}(H_{eff})$. From Equation (5), it can be seen that the spectral efficiency is limited by both the passive beamforming matrix and the precoding matrix. In order to maximize the achievable spectral efficiency of the system, the active and passive beamforming needs to be jointly optimized.

2.2. Problem Formulation

Based on the above system model, this subsection aims to maximize the spectral efficiency of the IRS-assisted MIMO communication system by jointly optimizing the precoding and passive beamforming, while the passive beamforming matrix needs to satisfy the single-mode discrete constraint of the IRS reflection elements and the precoding constraint mentioned previously. The mathematical description of the optimization problem is as follows:

$$\max_{F, \Phi} \log_2 \det \left(I_{N_r} + \frac{P}{\sigma^2 N_s} H_{eff}^H F F^H H_{eff} \right) \quad (6a)$$

$$s.t. \|F\|_F^2 = N_s \quad (6b)$$

$$\Phi = \text{diag}(e^{j\theta_1}, e^{j\theta_2}, \dots, e^{j\theta_M}) \quad (6c)$$

$$\theta_m \in \Gamma, m = 1, 2, \dots, M. \quad (6d)$$

where (6b) is the power constraint of the precoder, (6c) is the unit amplitude constraint of the IRS reflecting elements, and (6d) is the discrete constraint of the IRS reflection elements. We note that in the IRS with the discrete phase shifts setup, (6d) need not be considered. Since the objective function is non-convex and (6c) is a non-convex constraint, the optimization problem is a difficult multi-variate, mixed-integer nonconvex optimization problem. In addition, the precoding matrix F is coupled with the passive beamforming matrix, which makes the solution even more challenging.

3. Proposed Algorithm

In this section, we propose the MMSE-based algorithm for the ideal IRS with a continuous phase shifts setup and the multi-start stepwise optimization algorithm for the practical IRS with a discrete phase shifts setup, aiming to improve the system spectral efficiency and reduce the computational complexity.

3.1. MMSE-Based Algorithm for the Ideal IRS Setup

For an IRS-assisted millimeter-wave MIMO system with continuous phase shifters, the phase of the reflection elements of the IRS can be taken to any value of $[0, 2\pi]$. In this subsection, in order to maximize spectral efficiency, we propose an MMSE-based algorithm. Specifically, we first deflate the above problem into a simplified expression to facilitate the solution, and then we use the special structure of the passive beamforming matrix to derive its efficient closed-form solution based on the MMSE idea. Finally, the optimal precoding matrix is derived by performing the SVD on the effective channel and water-filling power allocation.

To obtain the desired passive beamforming matrix and precoding matrix, we let the effective matrix H_{eff}^H perform the following singular value decomposition:

$$H_{eff}^H = U\Lambda V^H = [U_1 \ U_2] \begin{bmatrix} \Lambda_1 & 0 \\ 0 & 0 \end{bmatrix} \begin{bmatrix} V_1^H \\ V_2^H \end{bmatrix} = U_1 \Lambda_1 V_1^H \quad (7)$$

where $U_1 \in \mathbb{C}^{N_r \times \text{rank}(H_{eff})}$ is the semi-unitary matrix satisfying $U_1^H U_1 = I$, $V_1 \in \mathbb{C}^{N_t \times \text{rank}(H_{eff})}$ is the semi-unitary matrix satisfying $V_1^H V_1 = I$, $\Lambda_1 = \text{diag}(\lambda_1^2, \lambda_2^2, \dots, \lambda_{\text{rank}(H_{eff})}^2) \in \mathbb{C}^{\text{rank}(H_{eff}) \times \text{rank}(H_{eff})}$ is the diagonal matrix, and $\lambda_1 \geq \lambda_2 \geq \dots \geq \lambda_{\text{rank}(H_{eff})}$. Then, when the passive beamforming matrix Φ is given, the ideal precoding matrix is obtained from the following equation:

$$F^{opt} = V_1 Q^{\frac{1}{2}} \quad (8)$$

where V_1 is the right singular matrix of H_{eff} and $Q = \text{diag}(p_1, p_2, \dots, p_{N_s}) \mathbb{C}^{N_s \times N_s}$ is the power allocation matrix, where p_i is the power allocated to the i -th data stream and $i = 1, 2, \dots, N_s$, satisfying $\sum_{i=1}^{N_s} p_i = N_s$ and $\{p_i\}_{i=1}^{N_s} \geq 0$. Substituting F^{opt} into the spectral efficiency objective function of Equation (5), we can obtain a spectral efficiency expression containing only the passive beamforming matrix

$$\begin{aligned} SE &= \log_2 \det \left(I_{N_r} + \frac{P}{\sigma^2 N_s} H_{eff}^H F F^H H_{eff} \right) \\ &= \log_2 \det \left(I_{N_r} + \frac{P}{\sigma^2 N_s} (U_1 \Lambda_1 V_1^H V_1 Q^{\frac{1}{2}} (V_1 Q^{\frac{1}{2}})^H (U_1 \Lambda_1 V_1^H)^H) \right) \\ &\stackrel{(a)}{=} \log_2 \det \left(I_{N_r} + \frac{P}{\sigma^2 N_s} \Lambda_1 Q \Lambda_1^H \right) \\ &\stackrel{(b)}{=} \sum_{i=1}^{N_s} \log_2 \left(1 + \frac{P \lambda_i^2 p_i}{N_s \sigma^2} \right) \end{aligned} \quad (9)$$

where (a) is due to $U_1^H U_1 = I$, $V_1^H V_1 = I$, and $|I + AB| = |I + BA|$, and (b) is due to the particularity that both Λ_1 and Q are diagonal matrices. According to Jensen's inequality [19], the following spectral efficiency deflation inequality exists over the downlink:

$$\sum_{i=1}^{N_s} \log_2 \left(1 + \frac{P \lambda_i^2 p_i}{N_s \sigma^2} \right) \stackrel{(c)}{\leq} N_s \log_2 \left(1 + \frac{P \sum_{i=1}^{N_s} \lambda_i^2}{N_s^2 \sigma^2} \right) = N_s \log_2 \left(1 + \frac{P \|H_{eff}\|_F^2}{N_s^2 \sigma^2} \right) \quad (10)$$

where (c) becomes the equality when, and only when, all singular values are equal. Inspired by (10), we propose to improve the spectral efficiency of the system by optimizing $\|H_{eff}\|_F^2$ under the constraint of (6b) and (6c) so as to obtain an approximate efficient closed-form solution of the reflection matrix Φ . We reformulate the problem as follows:

$$\begin{aligned} \max_{\Phi} & \|H_{eff}\|_F^2 = \text{Tr}(H_{eff} H_{eff}^H) = \text{Tr}(H_r \Phi G G^H \Phi^{-1} H_r^H) \\ \text{s.t.} & (6b), (6c) \end{aligned} \quad (11)$$

Notice that the problem is also a non-convex optimization problem, but the problem can be transformed into a minimum mean square error problem between the optimal solution and the actual solution. By using the special structure of its objective function, an efficient approximate closed solution can be derived. The specific algorithm is as seen in Equations (12)–(16).

Assuming that there is no amplitude constraint for the reflection elements of the IRS, the optimal solution in Equation (11) is as follows:

$$(H_r \Phi)_{opt} = W_{(1:N_r)}^H = W_{opt}^H \quad (12)$$

where $W_{(1:N_r)}$ is the left (right) singular matrix corresponding to the largest N_r singular value of $G G^H = W \Sigma W^H$, and the problem can be transformed into the problem of minimizing the Euclidean distance between the optimal solution and the actual solution, namely,

the minimum mean square error problem. From the matrix basics, it is known that the Euclidean distance of the matrix can be expressed in the form of a trace, and the equivalent objective problem is transformed into

$$\min_{\Phi} \text{Tr} \left[(W_{opt} - \Phi^{-1} H_r^H) (W_{opt} - \Phi^{-1} H_r^H)^H \right] \quad (13)$$

Since the objective problem in Equation (13) is convex function with respect to Φ , the non-convex optimization problem can be efficiently solved by transforming it into an easily solvable convex problem. The specific solution is as follows:

$$\begin{aligned} & \text{Tr} \left[(W_{opt} - \Phi^{-1} H_r^H) (W_{opt} - \Phi^{-1} H_r^H)^H \right] \\ &= \text{Tr} \left\{ \begin{bmatrix} w_1 - e^{-j\theta_1} \hat{h}_{r,1}^H \\ w_2 - e^{-j\theta_2} \hat{h}_{r,2}^H \\ w_3 - e^{-j\theta_3} \hat{h}_{r,3}^H \\ w_4 - e^{-j\theta_4} \hat{h}_{r,4}^H \end{bmatrix} \begin{bmatrix} w_1 - e^{-j\theta_1} \hat{h}_{r,1}^H \\ w_2 - e^{-j\theta_2} \hat{h}_{r,2}^H \\ w_3 - e^{-j\theta_3} \hat{h}_{r,3}^H \\ w_4 - e^{-j\theta_4} \hat{h}_{r,4}^H \end{bmatrix}^H \right\} \\ &= \sum_{m=1}^M \left\{ (w_m - e^{-j\theta_m} \hat{h}_{r,m}^H) (w_m - e^{-j\theta_m} \hat{h}_{r,m}^H)^H \right\} \\ &= \sum_{m=1}^M \left\{ (w_m w_m^H + \hat{h}_{r,m} \hat{h}_{r,m}^H - e^{-j\theta_m} \hat{h}_{r,m} w_m^H - e^{j\theta_m} w_m \hat{h}_{r,m}^H) \right\} \end{aligned} \quad (14)$$

where w_m is the m -th row vector of W_{opt} and $\hat{h}_{r,m}^H$ is the m -th row vector of H_r^H . Substituting $w_m \hat{h}_{r,m}^H \triangleq \alpha_m e^{j\beta_m}$ into Equation (14), the objective function of the MMSE problem can be transformed into

$$\sum_{m=1}^M \max_{\theta_m} (\alpha_m e^{-j(\beta_m + \theta_m)} + \alpha_m e^{j(\beta_m + \theta_m)}) \quad (15)$$

It is easy to obtain the optimal solution for θ_m , as follows:

$$\theta_m^* = -\beta_m = -\arg(w_m \hat{h}_{r,m}^H) \quad (16)$$

Next, we use the obtained optimal passive beamforming matrix to optimize the precoding matrix F . According to Equation (8), this problem is essentially a power allocation problem, which can be solved by the water-filling algorithm [20]. The power allocation process is similar to filling water into a pool of different grooves. Under the premise of a certain total power (water amount), more transmit power is allocated to the sub-paths with a large channel gain (deep grooves) and less transmit power is allocated to the sub-paths with a small channel gain (shallow groove) so as to obtain the maximum value of the sum of the spectral efficiency of each sub-path. Firstly, by introducing the Lagrange multiplier μ into Equation (9), we can obtain

$$L(\mu, p_i) = \sum_{i=1}^{N_s} \log_2 \left(1 + \frac{P \lambda_i^2 p_i}{N_s \sigma^2} \right) + \mu \left(N_s - \sum_{i=1}^{N_s} p_i \right) \quad (17)$$

By taking the partial derivative of the transmit power p_i for each sub-path and making the partial derivative equal to 0, we can obtain the optimal solution of p_i as $p_i^{opt} = \left(\frac{1}{\mu \ln 2} - \frac{N_s \sigma^2}{P \lambda_i^2} \right)^+$, where $(\cdot)^+ \triangleq \max\{\cdot, 0\}$. The Lagrange multiplier μ can be obtained by the power constraint, i.e., $\mu = \frac{1}{(N_s + \frac{N_s}{P} \sum_{i=1}^{N_s} \frac{\lambda_i^2}{\sigma^2}) \ln 2}$. If we let Q^{opt} be the optimal

power allocation matrix, we can obtain the optimal precoding matrix $F^{opt} = V_1(Q^{opt})^{\frac{1}{2}}$.

The above specific process is based on the MMSE scheme, and the algorithm flow is summarized in Algorithm 1.

Algorithm 1 MMSE-Based Algorithm

Input: $H_r = [h_{r,1} \ h_{r,2} \ \dots \ h_{r,N_r}]^H, G, P, \sigma$
Initialization: feasible $\Phi = I_M$
1: Perform SVD on GG^H as $GG^H = W\Sigma W^H$
2: Compute $W_{opt} = W_{(1:N_r)}$
3: **for** $i = 1 : M$, **do**
4: $w_m = W_{opt}(m, :)$
5: $\hat{h}_{r,m}^H = H_r^H(m, :)$
6: $\theta_m^* = -\arg(w_m \hat{h}_{r,m})$
7: **end for**
8: Compute $\Phi^{opt} = \text{diag}(e^{j\theta_1^*}, e^{j\theta_2^*}, \dots, e^{j\theta_M^*})$
9: Compute $H_{eff} = H_r \Phi^{opt} G$, and then perform SVD on it as $H_{eff}^H = U_1 \Lambda_1 V_1^H$
10: Water injection power allocation according to $p_i^{opt} = (\frac{1}{\mu \ln 2} - \frac{N_s \sigma^2}{P \lambda_i^2})^+$ and compute
 $F^{opt} = V_1(Q^{opt})^{\frac{1}{2}}$
Output: Φ^{opt} and F^{opt}

3.2. Multi-Start, Stepwise Optimization Algorithm for the Practical IRS Setup

For an IRS-assisted millimeter-wave MIMO system with discrete phase shifters, the phase of the reflection elements of the IRS can only take a certain number of discrete values. Therefore, the beamforming design of the IRS-assisted millimeter-wave MIMO system is a discrete constraint optimization problem. An intuitive idea is to quantify the obtained phase shift matrix for continuous constraints optimization to the nearest point in Γ based on the algorithm in Section 3.1, which can be obtained according to the following formula:

$$\theta_m^{opt} = \underset{\theta \in \Gamma}{\operatorname{argmin}} |\theta - \theta_m^*| \quad (18)$$

where θ_m^* is the optimal element of the passive beamforming matrix based on the MMSE algorithm in Section 3.1 and θ_m^{opt} is the corresponding optimal discrete phase shift value. However, this method of continuous phase shift quantization is bound to cause non-negligible errors at a low quantization accuracy, and so we must develop a new stepwise optimization scheme.

In order to maximize the spectral efficiency, we transform the optimization problem into a discrete phase search problem for IRS reflection elements. Although the classical traversal search algorithm can find the optimal solution, its complexity grows exponentially with the number of IRS reflection elements. For example, when the phase set contains 2^b different phases, there are $(2^b)^M$ different combinations of phase shift matrices. To reduce the complexity, we propose a stepwise optimization algorithm, which splits the overall design problem of the beamforming matrix Φ into the phase search problem of M reflection elements. When a particular reflection element phase is searched, the phase of other reflection elements is fixed, the selected phase is traversed from the set of optional phases and its objective function is calculated, and the phase corresponding to the optimal solution is selected.

Specifically, first of all, to avoid the algorithm from falling into a local optimal solution, we randomly generate N sets of reflection matrices through the following logistic chaos mapping sequence as the N starting points of the search, where the elements belong to $\Gamma = \{0, \Delta\theta, \dots, \Delta\theta(2^b - 1)\}$:

$$x(t+1) = ux(t)(1-x(t)) \quad (19)$$

where t denotes the number of chaotic iterations and $u \in (3.6, 4]$ is the chaotic parameter [21] which allows the mapping to be completely chaotic to make the search starting point diverse and uniform. The search is performed from each initial point to find the respective optimal solution, and then the best phase shift is selected from these optimal solutions as

the final optimization result, which can reduce the probability of the algorithm falling into local optimal solutions, to a certain extent.

Secondly, during the optimal phase search of the m -th reflection element, the phases of the $m + 1$ -th to M -th reflectors are fixed and correspond to the elements in $\bar{\Phi}$, and the phase of the m -th reflector is selected by traversal from $\Gamma = \{0, \Delta\theta, \dots, \Delta\theta(2^b - 1)\}$. The phases of the first to the $m - 1$ -th reflection elements are taken as the optimal values obtained in the previous iteration so that the $2^b - 1$ phase matrix is constructed and the corresponding spectral efficiency is calculated according to Equation (5), and the phase of the m -th reflection element is selected as the phase value corresponding to the maximum spectral efficiency. It should be noted that the design of the precoding matrix is referred to in 3.1, and the water-filling algorithm is used to implement the adaptive power allocation, which is not repeated here.

Finally, the optimal values of all reflection elements of Φ can be searched after M iterations. The algorithm only needs to calculate $2^b \times M$ times. The specific steps are summarized in Algorithm 2.

Algorithm 2 Multi-start, Stepwise Optimization Algorithm

Input: $H_r = [h_{r,1} \ h_{r,2} \ \dots \ h_{r,N_r}]^H$, G , P , σ , b

Initialization: $\Gamma = \{0, \Delta\theta, \dots, \Delta\theta(2^b - 1)\}$

1: Based on the logistic chaos mapping to randomly generate N different starting points

$\bar{\Phi} = [\bar{\theta}_1, \bar{\theta}_2, \dots, \bar{\theta}_M]$ from Γ , the search process for each starting point is as set out in **steps 2–9**.

2: **for** $i = 1 : M$, **do**

3: **for** $j = 1 : 2^b$, **do**

4: Set $\theta_i = \Gamma(j)$ and construct $[\theta_{i+1}, \theta_{i+2}, \dots, \theta_M]$ as $[\theta_{i+1}, \theta_{i+2}, \dots, \theta_M] = [\bar{\theta}_{i+1}, \bar{\theta}_{i+2}, \dots, \bar{\theta}_M]$

5: Set $\Phi^{(j)} = \text{diag}(\theta_1, \theta_2, \dots, \theta_M)$

6: Compute $H_{eff} = H_r \Phi^{(j)} G$ and perform SVD on it as $H_{eff}^H = U_1 \Lambda_1 V_1^H$

7: Water injection power allocation according to $p_i^{opt} = (\frac{1}{\mu \ln 2} - \frac{N_s \sigma^2}{P \lambda_i^2})^+$ and compute

$F^{opt} = V_1 (Q^{opt})^{\frac{1}{2}}$

8: Calculate $SE^{(j)}$, the spectral efficiency according to Equation (3)

9: **end for**

10: Select the maximum value of SE^{\max} among all $SE^{(j)}$

11: Set $\theta_i = \Gamma(\max)$

12: **end for**

13: $\Phi^{opt} = \text{diag}(e^{j\theta_1}, e^{j\theta_2}, \dots, e^{j\theta_M})$

Output: Φ^{opt}

4. Numerical Simulation Analysis

In this section, we simulate and analyze the beamforming optimization algorithm for the ideal IRS-assisted millimeter-wave MIMO system with a continuous phase shifts setup and the practical IRS-assisted millimeter-wave MIMO system with a discrete phase shifts setup, respectively, to verify the effectiveness of the algorithms proposed in this paper. The assumptions about ideal and practical IRSs are shown in Table 1. The main simulation parameters are set out in Table 2. MATLAB R2020a is used for simulation, and the results are based on 1000 random channel samples.

Table 1. The assumptions about ideal and practical IRSs.

Assumption	Ideal IRS	Practical IRS
Amplitude of IRS reflection element	1	1
Phase of IRS reflection element	$\theta_m \in [0, 2\pi]$	$\theta_m \in \{0, \Delta\theta, \dots, \Delta\theta(2^b - 1)\}$
Number of bits quantized (b)	none	[1, 5]

Table 2. The main simulation parameters.

Parameter	Value
Number of clusters (N_{cl})	3
Number of propagation paths per cluster (N_{ray})	2
Azimuth angles of arrival (AoA)	Uniform $[0, 2\pi]$
Azimuth angles of departure (AoD)	
Zenith angles of departure (ZoD)	
Number of transmitter antennas	16
Number of receiver antennas	4
Number of data streams	4
Spacing of BS antennas	0.5λ
Spacing of reflection elements	4λ
Average noise power	1
Interval of SNR	$[-10, 10]$

4.1. Simulation Results for the Ideal IRS Setup

For the ideal IRS with a continuous phase shifts setup, we compare the MMSE-based scheme proposed in this paper with the scheme of randomly generated IRS phases, the scheme of fixed power allocation (FPA), and the scheme of maximizing total channel power (Ctpm) [11] to verify the superiority of the algorithms proposed in this paper.

Figure 2 shows the SE of different algorithms with the increasing SNR in an IRS-assisted MIMO system with a continuous phase shifts setup, where $N_t = 16$, $M = 64$, $N_r = N_s = 4$, and the angle spread is 10° . It can be seen from Figure 2 that the spectral efficiency of all four schemes improves as the SNR increases. The spectral efficiency of the scheme proposed in this paper is improved by about 27% over that of the scheme of randomly generated IRS phases (random) under the same SNR condition, indicating that the result of the beamforming optimization affects the spectral efficiency of the system. Since the water-filling power allocation algorithm is an adaptive allocation of transmit power based on channel conditions, the proposed scheme is also superior to the FPA scheme. The Ctpm scheme obtains the local optimal solution by iteratively optimizing one reflection element and fixing other reflection elements through alternate optimization. The proposed scheme significantly improves the spectral performance, but at the expense of a certain complexity when the number of reflection elements, M , is large.

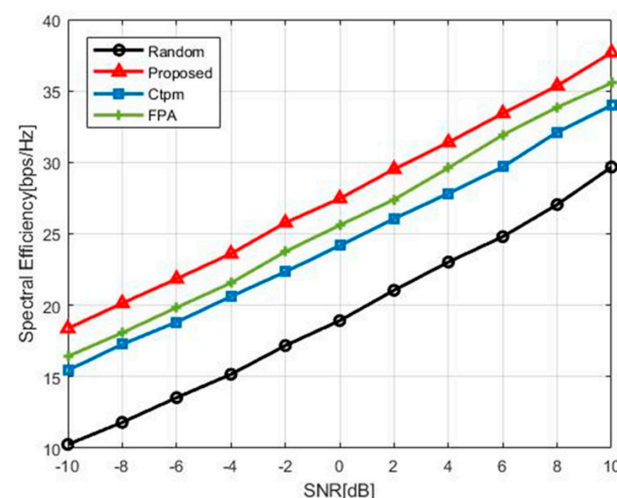


Figure 2. The spectral efficiency of an IRS-assisted MIMO system with a continuous phase shifts setup versus an SNR.

Figure 3 presents the SE of the different algorithms with the increasing IRS reflection elements in an IRS-assisted MIMO system with a continuous phase shifts setup, where $N_t = 16$, $N_r = N_s = 4$, $SNR = 0$ dB, and the angle spread is 10° . Apparently, as the number of reflection elements increases, the spectral efficiency of all schemes will improve. When the reflection element number is larger, the performance superiority of the proposed scheme will be more significant, and a higher gain can be achieved because each reflection element is designed to minimize the mean square error to obtain the approximate optimal solution.

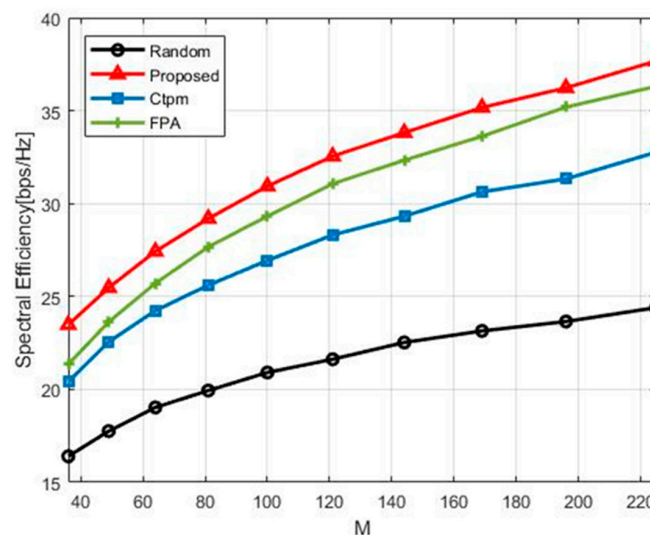


Figure 3. The spectral efficiency of an IRS-assisted MIMO system with a continuous phase shifts setup versus M .

Figure 4 shows the SE of the different algorithms with the increasing angle spread in an IRS-assisted MIMO system with a continuous phase shifts setup, where $N_t = 16$, $M = 64$, $N_r = N_s = 4$, and $SNR = 0$ dB. It is well known that millimeter-wave channels are sparse, and a sufficient ranking of BS–IRS channels can be guaranteed through deterministic scatterers only when the angle expansion is sufficient. The simulation results show that with the increase in the angle spread, the spectral efficiency will improve because a small angle spread and a small number of scatterers will lead to a lack of channel ranking, which will lead to the degradation of the MIMO system's performance. Under the same angle extension condition, the proposed scheme is always optimal.

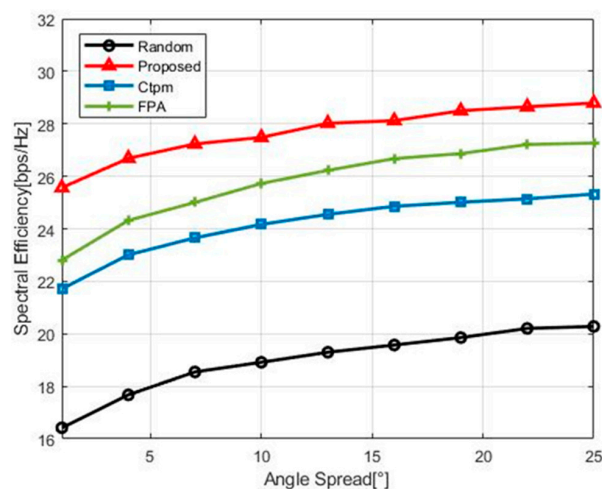


Figure 4. The spectral efficiency of an IRS-assisted MIMO system with a continuous phase shifts setup versus the angle spread.

4.2. Simulation Results for the Practical IRS Setup

For the practical IRS with a discrete phase shifts setup, we compare the multi-start, stepwise optimization algorithm proposed in this paper with the scheme of the randomly generated IRS phases, the MMSE-based continuous phase shift quantization scheme, and the local search (LS) scheme [22] at different bits to verify the superiority of the algorithms proposed in this paper.

As shown in Figure 5, we compare the SE of the different algorithms versus the SNR in an IRS-assisted MIMO system with a discrete phase shifts setup, where $N_t = 16$, $M = 64$, $N_r = N_s = 4$, the angle spread is 10° , and the number of bits quantized is 1 or 2. First, it can be seen that the spectral efficiency of the reflection elements using a 1-bit phase shifter is significantly higher than that of the random IRS phase scheme, indicating that even beamforming optimization using a very coarse phase shifter can improve the system's performance. Second, the use of a 2-bit phase shifter gives better results than the use of a 1-bit phase shifter because there is a coarse discrete phase shift and the multipath signal from the BS cannot be perfectly aligned in phase at the receiver, resulting in power loss. Finally, the multi-start, stepwise optimization algorithm proposed in this paper obtains higher gains compared to both the LS algorithm and the MMSE-based continuous quantization scheme.

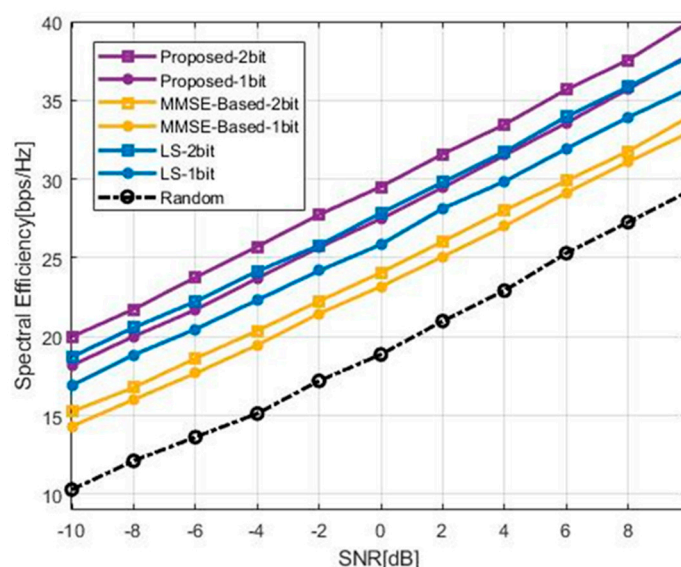


Figure 5. The spectral efficiency of an IRS-assisted MIMO system with a discrete phase shifts setup versus an SNR.

In Figure 6, we compare the SE of the different algorithms versus the IRS reflection elements in an IRS-assisted MIMO system with a discrete phase shifts setup, where $N_t = 16$, $N_r = N_s = 4$, the angle spread is 10° , the $SNR = 0dB$, and the number of bits quantized is 1 or 2. All the schemes show that the SE is improved as the number of reflecting elements, M , increases, but the rate of increase tends to be slow. When the number of reflecting elements is large enough, the high accuracy of the finite resolution phase can only be of a significant advantage.

Figure 7 depicts the SE of the different algorithms with the different number of bits quantized in an IRS-assisted MIMO system with a continuous phase shifts setup, where $N_t = 16$, $M = 64$, $N_r = N_s = 4$, and the angle spread is 10° . As the number of quantization bits increases, the SE will also improve, but the improvement effect after the accuracy reaches 3-bit is not obvious, which reveals that we only need to make the resolution to no more than 3-bit in engineering. If the accuracy is too high, it will sacrifice a certain cost overhead and the enhancement effect will be insignificant.

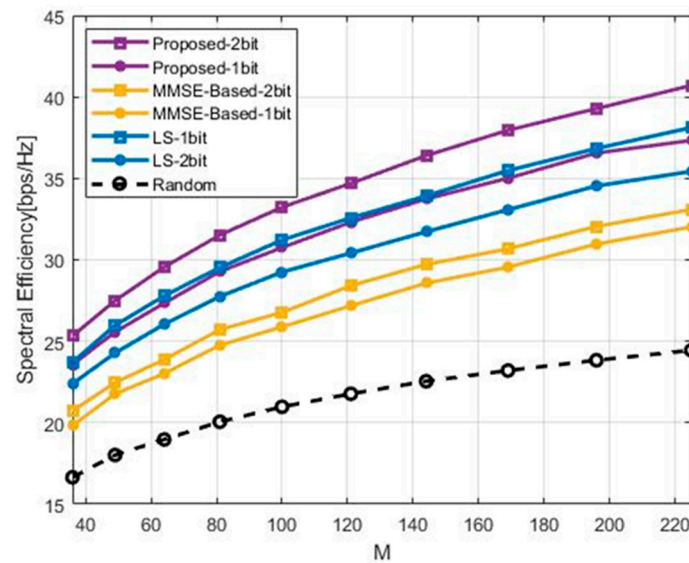


Figure 6. The spectral efficiency of an IRS-assisted MIMO system with a discrete phase shifts setup versus M .

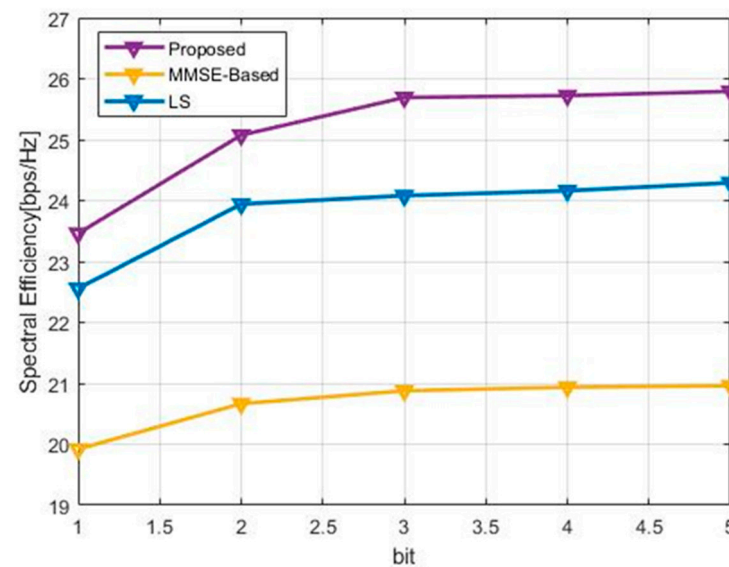


Figure 7. The spectral efficiency of an IRS-assisted MIMO system with a discrete phase shifts setup versus the number of bits quantized.

4.3. Computational Complexity Analysis

The computational complexities of the proposed schemes are presented in this subsection. For the ideal IRS setup, in the case of $M \gg N_t \geq N_r$, the complexity of some additions can be negligible, and the complexities of the MMSE-based algorithm can be simply expressed as $O(M^2(M + N_t))$. The computational complexity of the Ctpm algorithm is $O(N_t N_r (M + N_r) + N_t N_r M \gamma)$, where γ represents the number of iterations. It indicates that when M is large enough, the computational complexity of the MMSE-based algorithm will be large. For the practical IRS setup, the computational complexity of the classical traversal search algorithm is $O((2^b)^M)$, which grows exponentially with the number of IRS reflection elements. Compared to classical traversal search algorithm, the computational complexity of the multi-start, stepwise optimization algorithm and LS algorithm is only $O(2^b M)$. However, the performance of the multi-start, stepwise optimization algorithm is slightly better than that of the LS algorithm.

5. Conclusions

In this paper, we propose a beamforming optimization algorithm for a symmetry-based, IRS-assisted millimeter-wave point-to-point MIMO system, with the aim of improving the system's SE, while both the IRS with a continuous phase shifts setup and the IRS with a discrete phase shifts setup are investigated. For the IRS with a continuous phase shifts setup, a simplified approximate spectral efficiency optimization objective problem was obtained through Jensen's inequality scaling. The closed-form solution of the simplified problem was solved based on the MMSE algorithm and the optimal precoding was derived by applying SVD and water-filling power allocation. The simulation results show that our proposed MMSE-based scheme can achieve a better SE performance with moderate complexity compared with the random scheme, Ctpm scheme, and FPA scheme. For the IRS with a discrete phase shifts setup, we propose a multi-start, stepwise optimization algorithm to iterate the optimal discrete phase of the IRS, step-by-step. The extensive simulation results show that, compared with the random scheme, continuous phase-shift quantization scheme, and LS scheme, our beamforming scheme greatly reduces the complexity while improving the SE. In addition, it is shown that the IRS with a 3-bit quantizer can achieve a sufficient gain in SE with little performance degradation.

Author Contributions: Conceptualization, W.Z. and C.P.; methodology, W.Z., H.D. and Y.L.; software, W.Z. and Z.Z.; validation, W.Z. and Z.Z.; formal analysis, W.Z. and C.P.; investigation, W.Z. and G.L.; resources, W.Z.; data curation, W.Z.; writing—original draft preparation, W.Z. and C.P.; writing—review and editing, W.Z., H.D. and Y.L. All authors have read and agreed to the published version of the manuscript.

Funding: This research received no external funding.

Institutional Review Board Statement: Not applicable.

Informed Consent Statement: Not applicable.

Data Availability Statement: Not applicable.

Conflicts of Interest: The authors declare no conflict of interest.

References

- Chen, J.-C. Energy-Efficient Hybrid Precoding Design for Millimeter-Wave Massive MIMO Systems via Coordinate Update Algorithms. *IEEE Access* **2018**, *6*, 17361–17367. [\[CrossRef\]](#)
- Liu, G.; Deng, H.; Yang, K.; Zhu, Z.; Liu, J.; Dong, H. A New Design of Codebook for Hybrid Precoding in Millimeter-Wave Massive MIMO Systems. *Symmetry* **2021**, *13*, 743. [\[CrossRef\]](#)
- Wu, Q.; Zhang, R. Towards Smart and Reconfigurable Environment: Intelligent Reflecting Surface Aided Wireless Network. *IEEE Commun. Mag.* **2020**, *58*, 106–112. [\[CrossRef\]](#)
- Huang, C.; Hu, S.; Alexandropoulos, G.C.; Zappone, A.; Yuen, C.; Zhang, R.; Renzo, M.D.; Debbah, M. Holographic MIMO Surfaces for 6G Wireless Networks: Opportunities, Challenges, and Trends. *IEEE Wirel. Commun.* **2020**, *27*, 118–125. [\[CrossRef\]](#)
- Ur Rehman, H.; Bellili, F.; Mezghani, A.; Hossain, E. Joint Active and Passive Beamforming Design for IRS-Assisted Multi-User MIMO Systems: A VAMP-Based Approach. *IEEE Trans. Commun.* **2021**, *69*, 6734–6749. [\[CrossRef\]](#)
- Wu, Q.; Zhang, S.; Zheng, B.; You, C.; Zhang, R. Intelligent Reflecting Surface-Aided Wireless Communications: A Tutorial. *IEEE Trans. Commun.* **2021**, *69*, 3313–3351. [\[CrossRef\]](#)
- Yu, X.; Xu, D.; Sun, Y.; Ng, D.W.K.; Schober, R. Robust and Secure Wireless Communications via Intelligent Reflecting Surfaces. *IEEE J. Sel. Areas Commun.* **2020**, *38*, 2637–2652. [\[CrossRef\]](#)
- Guo, C.; Lu, Z.; Guo, Z.; Yang, F.; Ding, L. Maximum ergodic capacity of intelligent reflecting surface assisted MIMO wireless communication system. In Proceedings of the 14th EAI International Conference on Communications and Networking in China, Shanghai, China, 29 November–1 December 2019.
- Wu, Q.Q.; Zhang, R. Intelligent Reflecting Surface Enhanced Wireless Network: Joint Active and Passive Beamforming Design. In Proceedings of the 2018 IEEE Global Communications Conference (GLOBECOM), Abu Dhabi, United Arab Emirates, 9–13 December 2018.
- Guo, H.Y.; Liang, Y.C.; Chen, J.; Larsson, E.G. Weighted Sum-Rate Maximization for Reconfigurable Intelligent Surface Aided Wireless Networks. *IEEE Trans. Wirel. Commun.* **2020**, *19*, 3064–3076. [\[CrossRef\]](#)
- Zhang, S.W.; Zhang, R. Capacity Characterization for Intelligent Reflecting Surface Aided MIMO Communication. *IEEE J. Sel. Areas Commun.* **2020**, *38*, 1823–1838. [\[CrossRef\]](#)

12. Wu, Q.; Zhang, R. Beamforming Optimization for Intelligent Reflecting Surface with Discrete Phase Shifts. In Proceedings of the 2019 IEEE International Conference on Acoustics, Speech and Signal Processing (ICASSP), Brighton, UK, 12–17 May 2019.
13. Tan, X.; Sun, Z.; Jornet, J.M.; Patios, D. Increasing Indoor Spectrum Sharing Capacity using Smart Reflect-Array. In Proceedings of the 2016 IEEE International Conference on Communications (ICC), Kuala Lumpur, Malaysia, 22–27 May 2016.
14. Wang, P.L.; Fang, J.; Duan, H.P.; Li, H.B. Compressed Channel Estimation for Intelligent Reflecting Surface-Assisted Millimeter Wave Systems. *IEEE Signal Proc. Lett.* **2020**, *27*, 905–909. [[CrossRef](#)]
15. Wang, Z.R.; Liu, L.; Cui, S.G. Channel Estimation for Intelligent Reflecting Surface Assisted Multiuser Communications: Framework, Algorithms, and Analysis. *IEEE Trans. Wirel. Commun.* **2020**, *19*, 6607–6620. [[CrossRef](#)]
16. He, Z.Q.; Yuan, X.J. Cascaded Channel Estimation for Large Intelligent Metasurface Assisted Massive MIMO. *IEEE Wirel. Commun. Lett.* **2020**, *9*, 210–214. [[CrossRef](#)]
17. El Ayach, O.; Rajagopal, S.; Abu-Surra, S.; Pi, Z.Y.; Heath, R.W. Spatially Sparse Precoding in Millimeter Wave MIMO Systems. *IEEE Trans. Wirel. Commun.* **2014**, *13*, 1499–1513. [[CrossRef](#)]
18. Zhu, Z.X.; Deng, H.G.; Xu, F.X.; Zhang, W.J.; Liu, G.; Zhang, Y.H. Hybrid Precoding-Based Millimeter Wave Massive MIMO-NOMA Systems. *Symmetry* **2022**, *14*, 412. [[CrossRef](#)]
19. Wang, P.L.; Fang, J.; Dai, L.L.; Li, H.B. Joint Transceiver and Large Intelligent Surface Design for Massive MIMO mmWave Systems. *IEEE Trans. Wirel. Commun.* **2021**, *20*, 1052–1064. [[CrossRef](#)]
20. Di, B.Y.; Zhang, H.L.; Li, L.L.; Song, L.Y.; Li, Y.H.; Han, Z. Practical Hybrid Beamforming With Finite-Resolution Phase Shifters for Reconfigurable Intelligent Surface Based Multi-User Communications. *IEEE Trans. Veh. Technol.* **2020**, *69*, 4563–4568. [[CrossRef](#)]
21. Singh, N.; Sinha, A. Chaos-based secure communication system using logistic map. *Opt. Lasers Eng.* **2010**, *48*, 398–404. [[CrossRef](#)]
22. Chen, W.J.; Ma, X.Y.; Li, Z.X.; Kuang, N.Y. Sum-rate Maximization for Intelligent Reflecting Surface Based Terahertz Communication Systems. In Proceedings of the 2019 IEEE/CIC International Conference on Communications Workshops in China, Changchun, China, 11–13 August 2019; pp. 153–157.